Beads-on-string phenomena in wormlike micellar fluids

Michael C. Sostarecz and Andrew Belmonte
The W. G. Pritchard Laboratories, Department of Mathematics, Penn State University, University Park, Pennsylvania 16802

(Received 17 February 2004; accepted 10 June 2004; published online 19 July 2004)

We present experimental results on the dynamics of wormlike micellar filaments surrounded by an immiscible viscous bulk fluid. For certain concentrations, these filaments develop a beads-on-string structure previously observed only in polymer jets and filaments surrounded by air. By taking advantage of the longer time scales present in this experiment, we are able to quantify the evolution of individual beads. We also investigate the stability of these filaments and the robustness of the beads-on-string structure by stretching the filament within a rotating flow. © *2004 American Institute of Physics*. [DOI: 10.1063/1.1779672]

The beads-on-string instability is a well-known example of a uniquely viscoelastic phenomenon, in which a uniform filament develops into a series of large drops connected by thin threads.[1,2] Such beaded filaments have been observed in both jets[1–3] and stretched filaments[4,5] of polymer fluids in air, and have been reproduced numerically.[6–8] This general property of the resistance of polymer filaments to breakup is known as "spinnability." In contrast, jets and filaments of a Newtonian fluid break up rapidly into droplets by the surface tension driven Rayleigh instability.[9,10] A connection between Newtonian observations and polymer filament behavior is given by a nonlinear analysis using the Oldroyd-B constitutive equation,[6] which shows that the viscoelasticity caused by the addition of polymers has three effects: a delay of the onset of perturbations, faster perturbation growth, and the retardation of filament breakup due to the buildup of extensional stresses. A viscous exterior fluid has also been seen to significantly affect the pinch-off of Newtonian filaments.[11,12] Until now, the sole example of the beads-on-string phenomena within viscous fluids was reported by Chang *et al.*[7] In this experiment, a single viscoelastic bead was formed on a polymer filament in a Newtonian fluid of nearly the same density.

Another class of viscoelastic fluids are the so-called wormlike micellar fluids.[13] At the microscopic scale, these long tubular surfactant aggregates resemble their polymer counterparts. However, the aggregates continually break and re-form due to thermal fluctuations[14] and flow.[15] This added microscopic feature may be responsible for the interesting effects seen both rheologically[13,15–18] and hydrodynamically.[19–21] In fact, the oscillations observed in rising bubbles[21] and falling spheres[19] suggest that these micellar fluids may not be able to support large extensional stresses; the oscillations seem to be due to a wake instability.[21] Similarly, filaments of a wormlike micellar fluid have been seen to rupture suddenly when stretched in liquid bridges[18] or by a falling pendant drop.[20] It was therefore not obvious that a wormlike micellar fluid could sustain the extensional stresses needed to resist droplet formation[6,7] and produce the same beads-on-string phenomena seen in polymer fluids; see, however, Fig. 1.

In this Letter, we report the observation of the beads-on-string phenomena on a wormlike micellar filament in an immiscible viscous Newtonian oil. The filament is both produced and linearly stretched by a large pendant drop of the same fluid. The drop falls slowly through the oil due to the relatively low density difference ($\Delta\rho \simeq 0.03$ g/cm^3) and the viscosity of the bulk fluid. The beads that form appear to be similar to polymeric beads in air, though they are typically larger, and their dynamics occur on a much longer time scale; whereas the polymer filaments break in milliseconds or seconds, our experiments last on the order of minutes. Thus, we are able to take data without the use of a high-speed camera, and resolve the shape evolution of individual beads. We are also able to produce beads-on-a-string within an ongoing hydrodynamic flow, by injecting the wormlike micellar filament into a rotating viscous Newtonian oil.

The main experimental setup consists of a stationary clear rectangular cell filled with polydimethylsiloxane (PDMS) oil of viscosity 0.98 Pa s. The cell is a Plexiglas box, 42 cm in height, with cross-sectional area 5.7 cm $\times$ 6.3 cm. The micellar fluid is loaded at the top of the cell with a pipette (2 mm diameter) and pipetter. The pipette's position is fixed so that its tip is in the center of the cell, just touching the top surface of the oil. This prevents pinch-off at the orifice after the micellar fluid is injected. The wormlike micellar fluids used are aqueous solutions of equimolar concentrations (8–20 mM) of cetylpyridinium chloride (CPCl, surfactant) and sodium salicylate (NaSal, organic salt).[16,21] For a concentration of 10 mM, a relaxation time of $\lambda = 33$ s and a zero-shear viscosity of 4.8 Pa s were measured with a Rheometrics RFS-III rheometer in Couette geometry at 25 °C. Between the micellar solution and the exterior oil, a surface tension of 3.5 mN/m was measured by a pendant drop technique.[22] Due to the slowly changing filament surface, we ignore the kinetics of micellar adsorption and any dynamic surface tension effects. Video images were recorded with a charge coupled device (CCD) camera and a digital image processing system. Some still images were captured with a high-resolution color digital camera. All experimental data were taken at a room temperature of 21–23 °C.

The experiment starts when a volume (~1 ml) of the

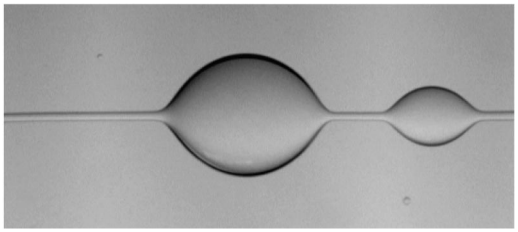

FIG. 1. Thinning filament of a wormlike micellar fluid (10 mM CPCl/NaSal) in PDMS oil displaying the beads-on-string phenomena. Image size is 0.6×1.3 cm^2.

heavier micellar fluid is injected at the top of the oil-filled cell, forming a pendant drop. As the pendant drop sinks at a constant terminal velocity ($U\simeq0.1$ cm/s), it stretches a filament that connects the drop to the pipette orifice, shown in Fig. 2(a) for 12 mM CPCl/NaSal. The filament remains uniform (radius $h_0\simeq0.06$ cm) over a length of more than 15 cm before local instabilities begin to develop close to the orifice; this occurs nearly 3 min after injection. The Deborah number based on the initial stretching of the filament is $\mathrm{De}=\lambda U/L=0.2$, where $L=L_{\mathrm{avg}}=17.5$ cm. Besides being the average length of the filament, L_{avg} is also the length of the filament when the initial beads-on-string perturbations begin to appear. In Fig. 2(b) the uniform filament gives way to the growing beads-on-string form. Much like a jet, time and space are related, since locations further from the pendant drop are older. In fact, this thinning filament might be seen as a reverse jet with its nozzle being the pendant drop. The beads-on-string instability develops further [Fig. 2(c)] into the classic form of large drops connected by thin threads [Fig. 2(d)], around the same time that the pendant drop hits the bottom of the Plexiglas cell ($t\approx6$ min). In the late stages

FIG. 2. Progression of the beads-on-string structure on a thinning filament of 12 mM CPCl/NaSal in PDMS oil. Each image size is 8.2×1.3 cm^2; times shown are (a) 3 min, (b) 4 min, (c) 5 min, and (d) 6 min.

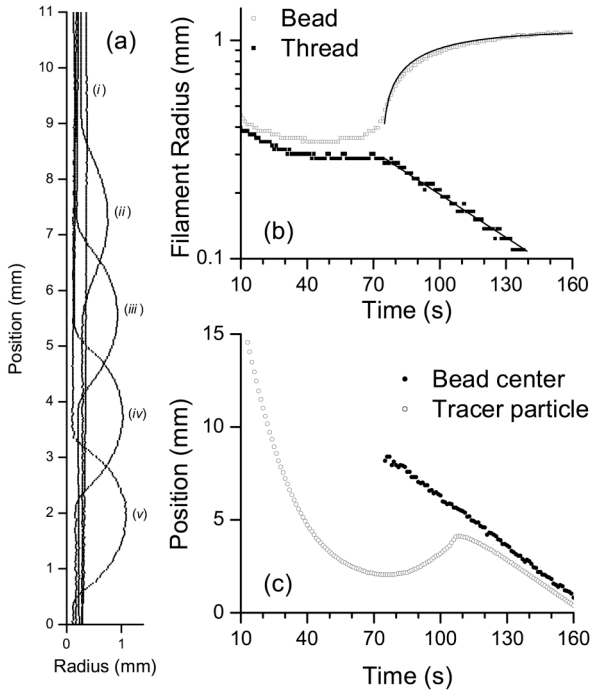

FIG. 3. Time evolution of a single bead on a filament of 8 mM CPCl/NaSal in PDMS oil. (a) Shape profiles at times (i) 65 s, (ii) 85 s, (iii) 105 s, (iv) 125 s, and (v) 145 s. (b) Maximum and minimum filament radius vs time. (c) Comparison of the bead center with a tracer particle.

of breakup ($t\approx8$ min), the connecting threads develop secondary beads.[3,8] Pinch-off finally occurs nearly 10 minutes after injection.

In Fig. 3, we analyze the profile of a bead as it forms on a stretched filament of 8 mM CPCl/NaSal. These curves were obtained from digitized images of the experiment with a resolution of 27.5 μm/pixel; the time is given relative to the moment that the initial pendant drop passed the midpoint of the cell ($t=0$). The development of a perturbation into a bead is shown in Fig. 3(a), in which the bead and filament are also falling due to gravity (0.01 cm/s, ten times slower than the pendant drop). In Fig. 3(b), we track the evolution of the maximum and minimum radii of the filament. The connecting thread exponentially decays with a rate close to $1/2\lambda$ during bead growth[9] [straight line in Fig. 3(b)]. Using this dependence and assuming that the fluid from the filament feeds a growing spherical bead, we obtain an analytic function for the bead height [curved line in Fig. 3(b)]. The lone free parameter, the distance between two beads, is fitted to $73h_0$, not far from the observed values of $51h_0$ [Fig. 3(a)] and $27h_0$ [Fig. 2(b)]. The Rayleigh prediction of $9h_0$ for an inviscid filament[9] would yield a smaller maximum bead height than observed experimentally.

Our ability to resolve the shape of the bead allows a test of various functional forms for its shape. In Fig. 4, a modified Gaussian, $h(z)=H+Ae^{-B|z|^3}$, compares well with three bead profiles at 30 s intervals. Here the bead's positions have been offset so that their center is at zero. This modified Gaussian does not work at later times, as the bead's profile approaches a spherical shape. Other shapes such as a true Gaussian or sech^2 do not fit well at even intermediate times

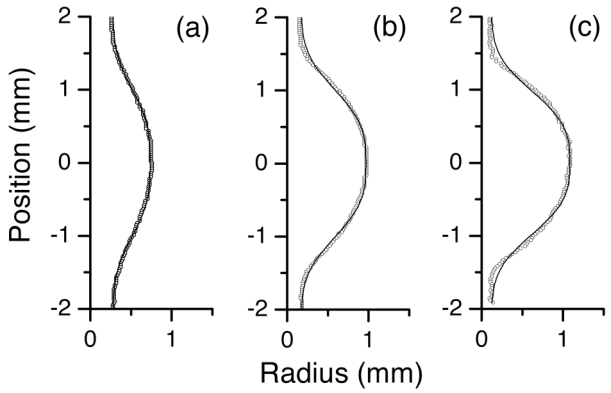

FIG. 4. Profile comparison of $h(z)=H+Ae^{-B|z|^3}$ with a growing bead on a filament of 8 mM CPCl/NaSal in PDMS oil. Times shown are (a) 85 s, (b) 115 s, and (c) 145 s.

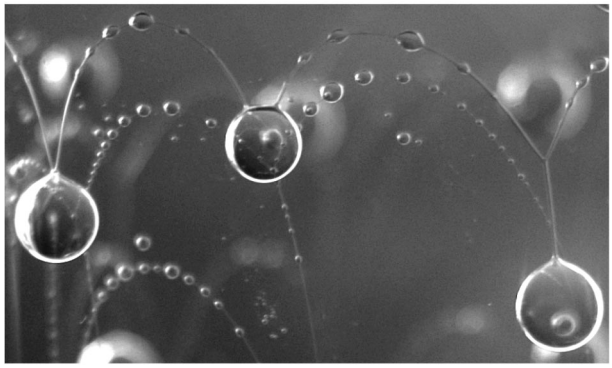

FIG. 6. Mobility of the connection points in the beads-on-string structure, for 10 mM CPCl/NaSal in PDMS oil, $\Omega=0.02$ Hz ($\Gamma\simeq 15$). Image size is 3.2×6.2 cm^2.

since they are too narrow at the peak and too gradual at the connection points.

We get an indication of the evolving velocity field by comparing the position of the bead's center with a tracer particle ($\sim$70 μm-diameter) located along the filament axis [Fig. 3(c)]. The tracer moves linearly down the filament during the initial stretching. Even before the bead begins to develop, the particle slows to a stop downstream of the bead's center. At nearly the same time that the bead appears ($t\approx 75$ s), the particle begins to move upstream with the fluid that feeds the developing bead. As the tracer reaches the apex of the connection point, it rapidly accelerates into the bead and continues to move slowly towards the center.[8] Its overall motion is down the filament, carried within the falling bead.

A new twist on the beaded filament experiment is shown in Fig. 5, in which a wormlike micellar filament of 10 mM CPCl/NaSal is injected into a steadily rotating tank filled with the same oil used previously.[23] The fluid is injected at a fixed rate of 1.3 ml/min with a syringe pump, through a 1 mm diameter pipette located 4.5 cm from the center of rotation. The rotation rate Ω ranges from 0.02 Hz to 0.25 Hz. Since the micellar fluid is almost neutrally buoyant, the rotation rate provides a direct and independent means of experimentally controlling the stretching of the filament, and thus the beads instability. This flow geometry allows us to fill the tank with a very long string of beads: Fig. 5 (0.25 Hz) shows one quadrant of a continuous domain of approximately 400 beads. The Deborah number here is $\mathrm{De}=\lambda\Omega\simeq 8.3$ and the Reynolds number based on the flow past the pipette is 0.08.

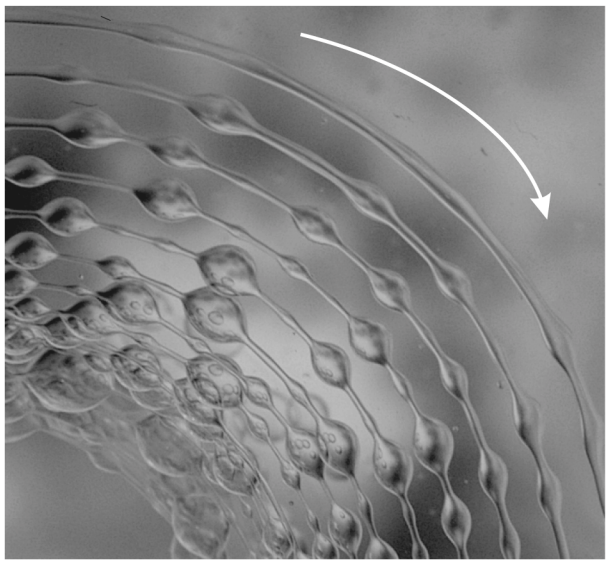

FIG. 5. Beads-on-a-string in a rotating geometry. 10 mM CPCl/NaSal in PDMS oil, $\Omega=0.25$ Hz. The arrow indicates the sense of rotation. Image size is 3.6×4.0 cm^2.

Once created, the viscoelastic beads-on-a-spiral structure begins to sink due to the slight density difference with the oil. From the side, the spiral forms a vase-like shape which is caused by a combination of the elasticity of the filament and the flow disturbance of the pipette tip in the rotating fluid. This is why Fig. 5 appears as concentric rings. The newer (outer) rings have just started to develop the perturbations while the beads-on-string structure appears later (inner rings). At the same rotation rate, the exterior flow causes an injected Newtonian filament (50/50 glycerol/water, $\Delta\rho=0.15$ g/cm^3, not shown) to take a similar vase-like shape. However, without viscoelasticity, it is comprised of individual droplets which have completely pinched off within 1 cm of the pipette tip.

For very slow rotation rates, it might be expected that a Rayleigh instability should break the micellar filament into droplets, as in the Newtonian case. However, in this case gravity is more dominant than the stretching caused by the rotating tank. As the Rayleigh instability begins, the thicker regions of the perturbation sink faster, causing the connecting filaments to stretch. This results in a striking cascade of the beads-on-string phenomenon occurring on arches connecting falling drops, as shown in Fig. 6 (0.02 Hz, De $=0.66$). We also note that the three large drops show that the filament-bead connection points are mobile—they move towards each other, meet at the top of the drop and merge. The right drop of Fig. 6 shows that this single junction can be pulled away from the drop into a "Y."

An indication of the cause of the stretching is given by the relative velocity ratio,

$$\Gamma = \frac{U_{\mathrm{rot}}}{U_{\mathrm{grav}}} = \frac{2\pi R\Omega}{U_{\mathrm{grav}}}, \tag{1}$$

which compares the rotational velocity with the filament's sinking velocity. At the extremes, $\Gamma \gg 1$ corresponds to a purely rotational stretching of the filament, while $\Gamma \ll 1$ implies that the drop is simply sinking in a quiescent fluid, as in the main experimental setup. This quantity can be obtained experimentally by measuring the amount of sinking in one rotation. For the tight spiral of Fig. 5, we have $\Gamma \simeq 430$, whereas the slow rotation of Fig. 6 has $\Gamma \simeq 15$. The transition between the two, judged by when the filament begins to bend within the first ring of the spiral, occurs at a critical value of $\Gamma_{\mathrm{crit}} = 105 \pm 15$.

We now discuss our observations. In other experimental studies in air, wormlike micellar filaments were observed to rupture suddenly and locally.[18,20] In contrast, the filaments here thin uniformly before developing a beads-on-string structure. In studies with an extensional rheometer, a liquid bridge was stretched exponentially in order to achieve a constant extension rate ($1.5\ \mathrm{s}^{-1} < \dot{\epsilon} < 3\ \mathrm{s}^{-1}$).[18] However, filaments following pendant drops are not stretched exponentially. Recently, extension rates of $0.05\ \mathrm{s}^{-1} < \dot{\epsilon} < 0.21\ \mathrm{s}^{-1}$ were estimated using

$$\dot{\epsilon}(t) = \frac{1}{L}\frac{dL}{dt}, \tag{2}$$

where L is the length of the filament.[20] The fact that these experiments did not produce beads may be due to a higher stretch rate. Using the terminal velocity of our pendant drop for dL/dt and $L = L_{\mathrm{avg}}$, we estimate an extension rate of $\dot{\epsilon} \simeq 0.006\ \mathrm{s}^{-1}$, much smaller than either of the above experiments.[18,20]

Not all concentrations of our wormlike micellar solution will produce the beads-on-string form. When concentration is increased slightly (20 mM CPCl/NaSal), a filament following a pendant drop pinches quickly (45 s), within 7 cm of the pipette. This effect looks similar to experiments of viscous Newtonian threads breaking in another viscous Newtonian fluid.[12] It has been seen previously that micelle concentration can affect free surface flows; air bubbles rising through wormlike micellar solutions (5–15 mM CPCl/NaSal) oscillated in both shape and velocity, while the oscillations cease for higher concentrations (16–24 mM CPCl/NaSal).[21] It is interesting that the regimes for the beads-on-string structure on filaments and the oscillations of rising bubbles appear to be related for these solutions. More experiments are being done to fully determine the effect of micelle concentration on filament and bead dynamics.

We have shown experimentally that a wormlike micellar filament can exhibit the beads-on-string instability: this is not limited to polymer fluids. By realizing this instability in a viscous medium, dynamics were observed that might have otherwise been lost at shorter time scales. Perhaps most striking is the robustness of the beads-on-string to an exterior rotating flow, showing that the connection points have mobility across the surface of the beads. In each case presented, the essential beads-on-string structure remains.

The authors thank J. R. Gladden, N. Z. Handzy, L. B. Smolka, and L. M. Walker for valuable discussions; G. McKinley for suggesting the use of volume conservation for Fig. 3, and R. Geist for experimental assistance. A.B. acknowledges support from The National Science Foundation (CAREER Award DMR-0094167).

[1] M. Goldin, J. Yerushalmi, R. Pfeffer, and R. Shinnar, "Breakup of a laminar capillary jet of a viscoelastic fluid," J. Fluid Mech. **38**, 689 (1969).
[2] A. L. Yarin, *Free Liquid Jets and Films: Hydrodynamics and Rheology* (Wiley, New York, 1993).
[3] Y. Christanti and L. M. Walker, "Surface tension driven jet break up of strain-hardening polymer solutions," J. Non-Newtonian Fluid Mech. **100**, 9 (2001).
[4] J. J. Cooper-White, J. E. Fagan, V. Tirtaatmadja, D. R. Lester, and D. V. Boger, "Drop formation dynamics of low-viscosity, elastic fluids," J. Non-Newtonian Fluid Mech. **106**, 29 (2002).
[5] L. B. Smolka, "On the motion of Newtonian and non-Newtonian liquid filaments: stretching, beading, blistering, pinching," Ph.D. thesis, Penn State University, 2002.
[6] D. W. Bousfield, R. Keunings, G. Marrucci, and M. M. Denn, "Nonlinear analysis of the surface tension driven breakup of viscoelastic filaments," J. Non-Newtonian Fluid Mech. **21**, 79 (1986).
[7] H.-C. Chang, E. A. Demekhin, and E. Kalaidin, "Iterated stretching of viscoelastic jets," Phys. Fluids **11**, 1717 (1999).
[8] J. Li and M. A. Fontelos, "Drop dynamics on the beads-on-string structure for viscoelastic jets: A numerical study," Phys. Fluids **15**, 922 (2003).
[9] J. Eggers, "Nonlinear dynamics and breakup of free-surface flows," Rev. Mod. Phys. **69**, 865 (1997).
[10] J. S. W. Rayleigh, "On the stability of a cylinder of viscous fluid under a capillary force," Philos. Mag. **34**, 145 (1892).
[11] S. Tomotika, "On the instability of a cylindrical thread of a viscous liquid surrounded by another viscous fluid," Proc. R. Soc. London, Ser. A **150**, 322 (1935).
[12] I. Cohen and S. R. Nagel, "Testing for scaling behavior dependence on geometrical and fluid parameters in the two fluid snap-off problem," Phys. Fluids **13**, 3533 (2001).
[13] R. G. Larson, *The Structure and Rheology of Complex Fluids* (Oxford University Press, New York, 1999).
[14] M. E. Cates and S. J. Candau, "Statics and dynamics of worm-like surfactant micelles," J. Phys.: Condens. Matter **2**, 6869 (1990).
[15] E. K. Wheeler, P. Fischer, and G. G. Fuller, "Time-periodic flow induced structures and instabilities in a viscoelastic surfactant solution," J. Non-Newtonian Fluid Mech. **75**, 193 (1998).
[16] H. Rchage and H. Hoffmann, "Rheological properties of viscoelastic surfactant systems," J. Phys. Chem. **92**, 4712 (1988).
[17] L. M. Walker, P. Moldenaers, and J.-P. Berret, "Macroscopic response of wormlike micelles to elongational flow," Langmuir **12**, 6309 (1996).
[18] J. P. Rothstein, "Transient extensional rheology of wormlike micelle solutions," J. Rheol. **47**, 1227 (2003).
[19] A. Jayaraman and A. Belmonte, "Oscillations of a solid sphere falling through a wormlike micellar fluid," Phys. Rev. E **67**, 065301 (2003).
[20] L. B. Smolka and A. Belmonte, "Drop pinch-off and filament dynamics of wormlike micellar fluids," J. Non-Newtonian Fluid Mech. **115**, 1 (2003).
[21] N. Z. Handzy and A. Belmonte, "Oscillatory rise of bubbles in wormlike micellar fluids with different microstructures," Phys. Rev. Lett. **92**, 124501 (2004).
[22] D. S. Ambwani and T. Fort, "Pendant drop technique for measuring liquid boundary tensions," in *Surface and Colloid Science*, Experimental Methods, edited by R. J. Good and R. R. Stromberg (Plenum, New York, 1979), Vol. 11, pp. 93–118.
[23] The Plexiglas tank has cross section $18 \times 18\ \mathrm{cm}^2$ and is filled to a depth of 9 cm.